Could Dissecting the Molecular Framework of β-Lactam Integrin Ligands Enhance Selectivity?

Could dissecting the molecular framework of β-lactam integrin ligands enhance selectivity?

Giulia Martelli,[†≠] Monica Baiula,[‡≠] Alberto Caligiana,[‡] Paola Galletti,[†] Luca Gentilucci,[†] Roberto Artali,[&] Santi Spampinato, *[‡] Daria Giacomini, *[†]

[†] Department of Chemistry "G. Ciamician", University of Bologna, Via Selmi 2, 40126 Bologna, Italy.

[‡] Department of Pharmacy and Biotechnology, University of Bologna, Via Irnerio, 48, 40126, Bologna, Italy

[&] Scientia Advice, 20832, Desio, Monza and Brianza, Italy

KEYWORDS Lactams, integrins, cell adhesion, agonist, antagonist, azetidinones, peptidomimetics.

ABSTRACT: By dissecting the structure of β-lactam-based ligands, a new series of compounds was designed, synthesized, and evaluated toward integrin $\alpha_v\beta_3$ $\alpha_5\beta_1$, and $\alpha_4\beta_1$. New selective ligands with antagonist or agonist activities of cell adhesion in the nanomolar range were obtained. The best agonist molecules induced significant adhesion of SK-MEL-24 cells and Saos-2 cells, as a valuable model for osteoblast adhesion. These data could lead to the development of new agents to improve cellular osseointegration and bone regeneration. Molecular modeling studies on prototypic compounds and $\alpha_v\beta_3$ or $\alpha_5\beta_1$ integrins supported that ligand carboxylate fixing to the MIDAS in the β-subunit can be sufficient for binding the receptors, while the aryl side chains play a role in determining the selectivity as well as agonism vs antagonism.

INTRODUCTION

Integrins are membrane receptors that play an important role in the regulation of fundamental functions such as development, cell adhesion, and migration.[1,2] They also participate in platelet adhesion[3] and in the immune response, considering their presence in leukocyte cells by modulating specific intracellular signaling pathways.[4] Integrins are also implicated in the progression and metastasis of certain tumors.[5,6] Activation of integrins can occur by binding extracellular ligands (outside-in signaling) or intracellular activation of integrin tails (inside-out signaling). The interaction of integrins with extracellular ligands could enable or preclude cellular signaling that controls cell processes such as cell shape, growth, and differentiation.[7] Ligand binding may influence integrin conformation from a low inactive state to higher active states.[8,9] Several studies have examined integrin ligands acting as antagonists that block the interaction between integrin and its endogenous ligands, such as antibodies, peptides, or small organic molecules.[10] Preclinical studies suggest that several integrin antagonists might be useful to suppress tumor angiogenesis and growth either alone, or in combination with current cancer therapeutics.[11] Less attention has been paid to the ligands that activate integrins for the possible activation of angiogenesis and tumor growth. However, it has been recently recognized that integrin agonists could lead to benefits by increasing integrin-dependent cell adhesion rather than inhibiting it.[12,13]

Our previous studies provided a novel series of β-lactam-based molecules that were designed to target different integrins, mainly RGD-binding and leukocyte-integrins (selected molecules **A-F** Chart 1).[14, 15]

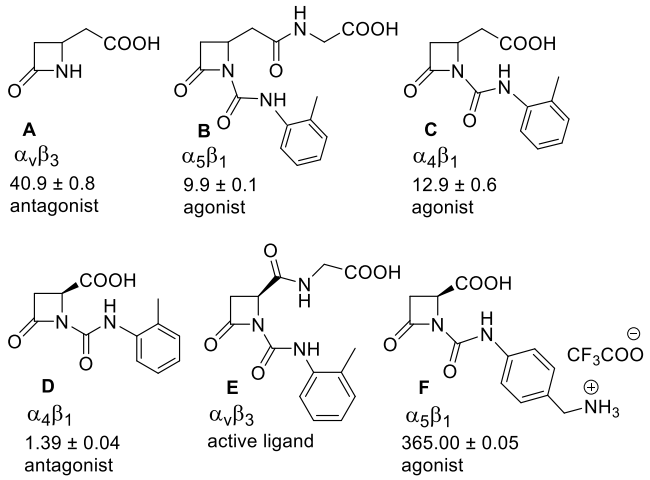

Chart 1. β-Lactam compounds previously reported (**A-F,** ref. 15) and selected for the design of the new molecules.

We identified selective and potent ligands able to modulate differently cell signaling pathways: some molecules acted as agonists, hence promoting cell adhesion and intracellular signaling activation, while others were antagonists inhibiting integrin-dependent cell functions. Despite the selective binding and valuable potency of some of the reported molecules, it is relevant to recognize the structural requirements to address the selectivity and the agonist/antagonist behavior of new integrin ligands.

Thus, a series of new ligands was designed and obtained by dissecting the structures of some compounds that were previously synthesized (Chart 2).

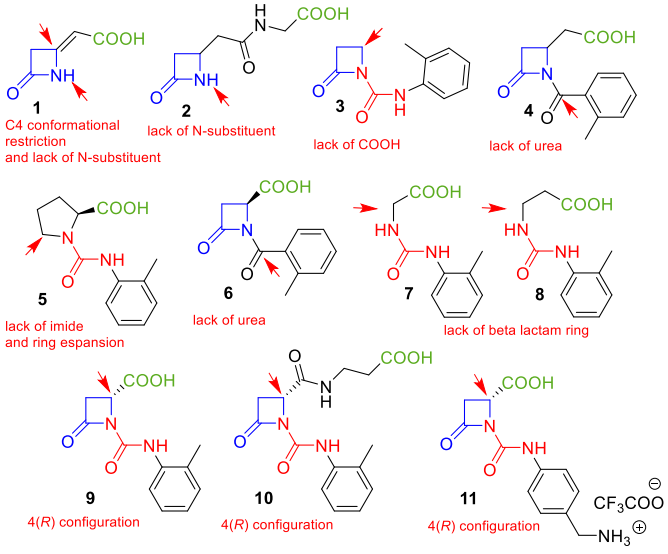

Chart 2. Structure-based design of new molecules (**1-11**). The arrows indicate the modified positions.

The novel compounds were deprived of some functional groups or destructured from their cyclic scaffold compared to those already reported. The new series of molecules was tested toward integrins $\alpha_v\beta_3$, $\alpha_5\beta_1$, and $\alpha_4\beta_1$, the three main receptors targeted by the previously reported β-lactam ligands through cell adhesion assays, competitive solid-phase binding assays, and integrin-mediated intracellular signaling analysis. Some derivatives were very active ligands in the nanomolar range despite the extent of chemical manipulation.

RESULTS

Synthesis of new compounds. The synthetic strategies adopted for the new β-lactams are reported in Schemes 1-3. The synthesis of derivatives **1**, **2** and **4** share the commercially available 4-acetoxyazetidin-2-one as the starting material (Scheme 1). Compound **1**, characterized by a double bond directly linked to the ring,[16] was obtained as previously described.[17]

Compound **15** was obtained by hydrogenolysis of **13** and further coupling with glycine benzylester to achieve **16**. The benzyl ester was finally removed to give compound **2**. Starting from the benzyl ester of the commercially available 4-carboxylic-azetidin-2-one, intermediate **12** was obtained by acylation with *o*-toluoylchloride, and subsequent ester deprotection by hydrogenolysis to give carboxylic acid **6** (Scheme 1).

Scheme 1. Synthesis of compounds **1-4**, and **6**[a]

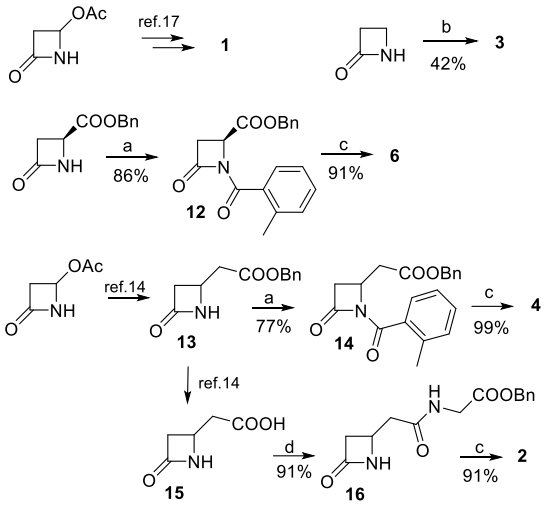

[a] Reagents and conditions: a) o-toluoylchloride, TEA, DMAP, CH_2Cl_2, 0 °C then rt, 18 h; b) *o*-tolylisocyanate, NaHMDSA, THF, -78 °C, 1 h; c) H_2, Pd/C (10%), THF/CH_3OH 1:1, rt, 2 h; d) DCC, TEA, DMAP, glycine benzylester·HCl, CH_2Cl_2, 0 °C to rt, 16 h.

Scheme 2. Synthesis of compounds **5, 7,** and **8**[a]

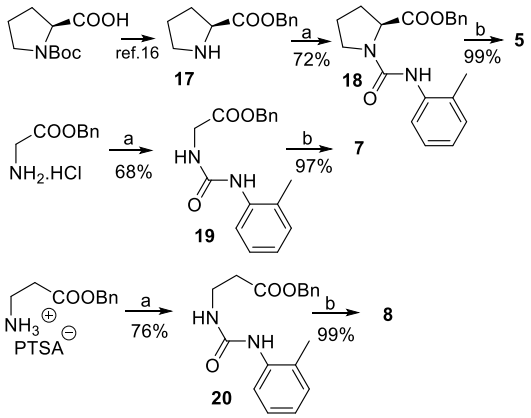

[a] Reagents and conditions: a) *o*-tolylisocyanate, TEA, CH_2Cl_2, rt, 4 h; b) H_2, Pd/C 10%, THF/ CH_3OH 1:1, rt, 2 h.

Compound **3** was obtained starting from the commercially available 2-azetidinone by *o*-tolylisocyanate acylation at low temperature (Scheme 1). Compound **17** was obtained from *N*-Boc-L-proline following a previously reported procedure:[18] acylation with *o*-tolylisocyanate gave **18** and a final hydrogenolysis quantitatively yielded target compound **5** (Scheme 2). Linear derivatives **7** and **8** were obtained similarly starting from glycine and β-alanine

Table 1. Effects of β-lactam compounds **1-11** on RGD-binding- and leukocyte-integrin-mediated cell adhesion. Data are presented as EC_{50} for agonists, and as IC_{50} for antagonists (nM).[a,b]

comp. number	SK-MEL-24/ FN $\alpha_v\beta_3$	K562/FN $\alpha_5\beta_1$	Jurkat/ VCAM-1 $\alpha_4\beta_1$	comp. number	SK-MEL-24/FN $\alpha_v\beta_3$	K562/FN $\alpha_5\beta_1$	Jurkat/VCAM-1 $\alpha_4\beta_1$
1	75.6 ± 7.8 agonist	>5000	255 ± 26 agonist	**10**	>5000	96.9 ± 2.3 antagonist	>5000
2	>5000	1110 ± 111 antagonist	>5000	**11**	>5000	>5000	>5000
3	>5000	>5000	976 ± 54 agonist				
4	>5000	419 ± 31 antagonist	>5000	**A**	40.9 ± 0.8 antagonist	1031 ± 35 agonist	> 5000
5	2880 ± 69 agonist	140 ± 15 agonist	10.0 ± 2.1 agonist	**B**	> 5000	9.9 ± 0.1 agonist	> 5000
6	>5000	41.5 ± 2.3 antagonist	>5000	**C**	> 5000	> 5000	12.9 ± 0.6 agonist
7	84.8 ± 4.5 agonist	3512 ± 48 antagonist	>5000	**D**	352 ± 7 antagonist	158 ± 4 antagonist	1.39 ± 0.04 antagonist
8	29.9 ± 5.9 agonist	>5000	>5000	**E**	active ligand	>5000	>5000
9	>5000	>5000	>5000	**F**	> 5000	365.00 ± 0.05 agonist	> 5000

[a]Cell adhesion mediated by $\alpha_v\beta_3$ was measured by assaying SK-MEL-24 cells adhesion to FN; by $\alpha_5\beta_1$ assaying K562 cell adhesion to FN; by $\alpha_4\beta_1$ evaluating Jurkat cell adhesion to VCAM-1. [b]Values represent the mean ± SD, n=3.

Scheme 3. Synthesis of compounds **9, 10,** and **11**[a]

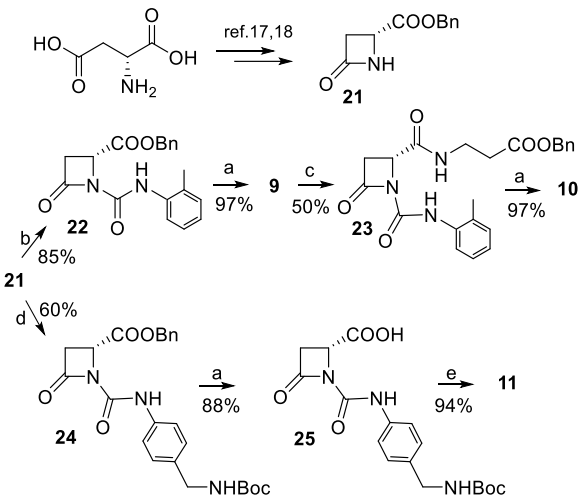

[a] Reagents and conditions: a) H_2, Pd/C (10%), THF/CH_3OH 1:1, rt, 2 h; b) o-tolylisocyanate, TEA, CH_2Cl_2, rt, 4 h; c) oxalylchloride, TEA, CH_2Cl_2, β-alanine benzylester·PTSA, DMAP, rt, 16 h; d) NaHMDSA, tert-butyl 4-isocyanatobenzylcarbamate **26**, THF, -78 °C, 1 h; e) TFA, CH_2Cl_2, 0 °C then rt, 6 h.

benzyl esters through the acylated intermediates **19** and **20**, respectively, and their subsequent hydrogenolysis (Scheme 2). Azetidinone benzyl ester **21** was obtained from D-aspartic acid in a two-step procedure: formation of the di-benzylester[19] and cyclization with *tert*-butylmagnesium chloride[20] (Scheme 3). β-Lactam **21** was then exploited as a starting material for the D-β-lactam derivatives **9**-**11**. Acylation of **21** with *o*-tolylisocyanate gave **22**, and subsequent hydrogenolysis yielded **9**; then, coupling with β-alanine benzylester gave **23**, followed by a final hydrogenolysis to obtain **10** (Scheme 3). Finally, intermediate **24** was obtained from **21** by condensation with *tert*-butyl(4-isocyanatobenzylcarbamate) **26** prepared *in situ* with triphosgene, TEA and 4-aminobenzylamine.[14, 17] Hydrogenolysis of **24** gave acid **25** and the final deprotection of the *N*-Boc group yielded **11** (Scheme 3).

Pharmacology. The ability of the new ligands to modulate cell adhesion was assayed using different cell lines: SK-MEL-24 (expressing $\alpha_v\beta_3$),[21] K562 (mainly expressing $\alpha_5\beta_1$),[22] and Jurkat E6.1 (expressing $\alpha_4\beta_1$)[15]. The results of the cell adhesion assays with compounds **1**-**11** are summarized in Table 1. Ligands that inhibit the cell adhesion promoted by fibronectin (FN) or VCAM-1 are referred to as antagonists whereas compounds that increase the cell adhesion are defined agonists. For comparison purposes, cell adhesion data of selected β-lactam ligands **A-F** previously studied[15] have been added to Table 1. Further characterization to evaluate the integrin affinity of the most interesting compounds in cell adhesion assays was performed with a solid-phase competitive integrin binding

assay for the integrins $\alpha_v\beta_3$ and $\alpha_5\beta_1$ and with a scintillation proximity-binding assay (SPA) for $\alpha_4\beta_1$[15] (Table 2).

Proline derivative **5** showed the most potent agonist activity toward $\alpha_4\beta_1$ (EC_{50} = 10.0 nM) and displayed an excellent affinity for this integrin as measured by SPA (Table 2). In addition, compound **5**, which was previously coated to the wells by passive absorption, slightly increased Jurkat cell adhesion compared to VCAM-1 (Figure 1A). Neutralizing antibodies to the α_4 integrin subunit (10 μg/mL) reduced the cell adhesion mediated by compound **5** (10 μg/mL) to Jurkat cells (data not shown). Regarding integrin $\alpha_5\beta_1$, compounds **6** and **10** behaved as selective antagonists (IC_{50} of 41.5 and 96.9 nM, respectively). In contrast, compound **5** favored $\alpha_5\beta_1$-mediated cell adhesion with an EC_{50} in the submicromolar range, and this result was confirmed by the affinity of compound **5** for this integrin (Table 2). Compounds **1**, **7**, and **8** increased cell adhesion mediated by integrin $\alpha_v\beta_3$ with excellent potency (EC_{50} 75.6, 84.8, and 29.9 nM, respectively), whereas **5** behaved as a weak agonist. Furthermore, **7** and **8** emerged as selective ligands for the $\alpha_v\beta_3$ integrin.

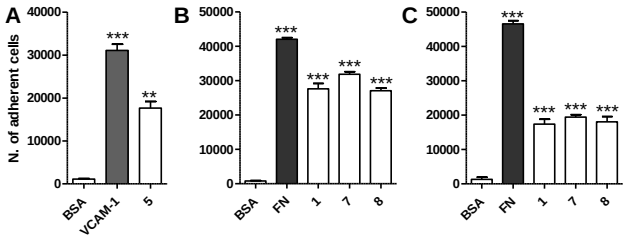

Figure 1. Jurkat (A), SK-MEL-24 (B) and Saos-2 (C) cell adhesion to wells coated with VCAM-1, FN, the most effective agonists (**1**, **5**, **7** and **8)** or BSA as controls. Values as mean ± SEM from three independent experiments carried out in quadruplicate. **p<0.01; ***p<0.001 vs to BSA-coated wells (Newman−Keuls test after ANOVA).

The most active compounds **1**, **4-8,** and **10** were further evaluated by solid-phase competitive binding assays for $\alpha_v\beta_3$ and $\alpha_5\beta_1$ integrins, or with SPA for $\alpha_4\beta_1$ (Table 2). The affinity data are in complete agreement with the data obtained in the adhesion tests, and confirmed that compounds **7** and **8** were the best and most selective ligands for $\alpha_v\beta_3$, compound **10** was the best and most selective for $\alpha_5\beta_1$, and compound **5** was the best ligand for $\alpha_4\beta_1$ but not selective.

To better characterize the $\alpha_v\beta_3$ agonists **1**, **7** and **8**, we investigated their ability to modulate adhesion of Saos-2 cells, a human osteoblast-like cell expressing $\alpha_v\beta_3$ and $\alpha_5\beta_1$ integrins, considered a valuable *in vitro* model to study osteoblast adhesion and osseointegration of implants in dentistry and orthopedics.[23-25]

The use of $\alpha_v\beta_3$ and $\alpha_5\beta_1$ integrin agonists has been described as a feasible and powerful strategy to improve osteoblast adhesion because it can mimic the extracellular matrix of the bone.[23-25] β-Lactams **1**, **7** and **8** were able to increase Saos-2 cell adhesion to FN in the nanomolar range (**1** EC_{50}= 154 ± 35 nM; **7** EC_{50}=299 ± 54 nM; **8** EC50 = 984 ± 72 nM), although they displayed a lower potency than those obtained in SK-MEL-24 cells.

Table 2. IC_{50} values (nM)[a] of compounds **1**, **4-8**, and **10** on $\alpha_v\beta_3$, $\alpha_5\beta_1$, and $\alpha_4\beta_1$ integrins.

Compd.	$\alpha_v\beta_3$	$\alpha_5\beta_1$	$\alpha_4\beta_1$
1	29.0 ± 2.6	>1000	294 ± 28
4	>1000	409 ± 33	>1000
5	>1000	136 ± 16	18.9 ± 2.1
6	>1000	59.3 ± 7.1	>1000
7	3.4 ± 0.8	>1000	>1000
8	9.5 ± 1.9	>1000	>1000
10	>1000	11.9 ± 2.5	>1000

[a] IC_{50} for $\alpha_v\beta_3$, $\alpha_5\beta_1$ was evaluated by competitive solid-phase binding assay to FN. IC_{50} for $\alpha_4\beta_1$ was determined by SPA. Values are the mean ± SEM (n=3).

Moreover, **1**, **7** and **8**, which had been previously coated to the wells by passive absorption, induced significant adhesion of SK-MEL-24 and Saos-2 cells in the absence of FN (Figure 1 B and C, respectively).

The addition of a neutralizing antibody to the α_v subunit added to SK-MEL-24 or Saos-2 cells 10 min prior to the addition of compounds **1**, **7** and **8** (10 μg/mL) strongly reduced the adhesion (data not shown), indicating that these compounds specifically mediate the process through $\alpha_v\beta_3$ integrins.

To further characterize the most effective compounds evaluated in the integrin-mediated cell adhesion assays, intracellular signaling activation was investigated.

Extracellular signal-regulated kinase 1 and 2 (ERK1/2) phosphorylation was quantified as evidence of the intracellular signal derived by integrin-extracellular matrix component interactions.[15] As ERK1/2 signaling pathway is impaired in SK-MEL-24 cells,[26] we transfected HEK293 cells, which do not express $\alpha_v\beta_3$ integrin,[27-29] with plasmids coding for α_v and β_3 subunits (HEK293+ $\alpha_v\beta_3$) in order to study $\alpha_v\beta_3$-mediated ERK1/2 phosphorylation.

Positive controls for signaling activation were FN for $\alpha_v\beta_3$ and $\alpha_5\beta_1$ and VCAM-1 for $\alpha_4\beta_1$; as expected both endogenous agonists were able to induce ERK1/2 phosphorylation when compared with vehicle-treated cells or with not transfected HEK293 cells (adopted as negative control for HEK293+$\alpha_v\beta_3$ cells) (Figure 2).

A significant increase in ERK1/2 phosphorylation was induced by compounds **1**, **7**, and **8** in HEK+$\alpha_v\beta_3$ cells (Figure 2A); however the compounds were not able to activate ERK1/2 signaling in not transfected HEK293 cells (data not shown). Regarding integrin $\alpha_4\beta_1$, compound **5** confirmed its agonist effect by increasing the integrin-mediated intracellular signaling activation in a concentration-dependent manner in Jurkat cells (Figure 2B). In contrast, antagonist compound **6**, active towards $\alpha_5\beta_1$, prevented FN-induced ERK1/2 phosphorylation in K562 cells (Figure 2C). On the basis of these data, we can conclude that compounds acting as agonists increase integrin-mediated cell adhesion, promote integrin mediated-intracellular signaling, mimicking the behavior of endogenous agonists, like fibronectin or VCAM-1.

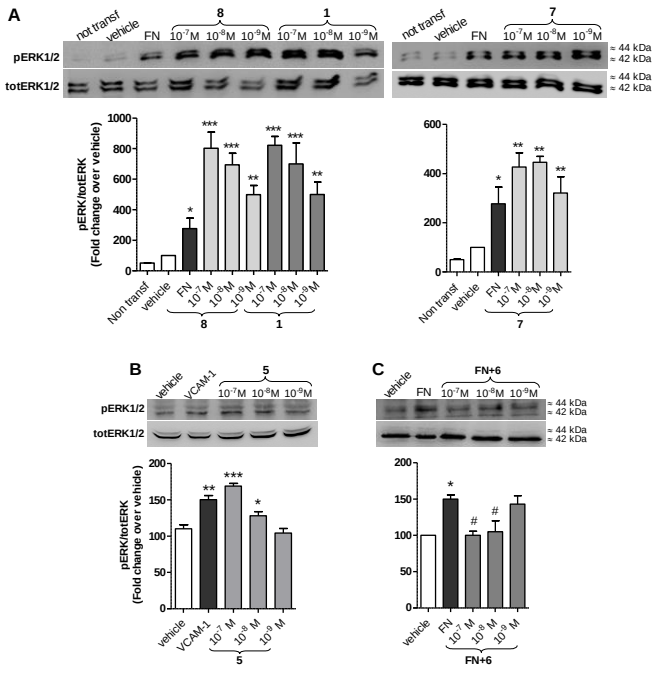

Figure 2. Concentration dependent effects of new β-lactam ligands on integrin-mediated intracellular signaling activation. (A) Compounds **8**, **1**, and **7** increased ERK1/2 phosphorylation in HEK293+$\alpha_v\beta_3$ cells; (B) compound **5** activated intracellular signaling in Jurkat cells expressing $\alpha_4\beta_1$; (C) compound **6** prevented FN-induced ERK1/2 phosphorylation in K562 cells expressing $\alpha_5\beta_1$. Not transf: not transfected HEK293 cells. Densitometric analysis of the bands is reported (mean ± SEM; n=5). *p<0.05, **p<0.01, ***p<0.001 vs vehicle; #p<0.05 vs FN (Newman-Keuls test after ANOVA).

Conversely, ligands acting as antagonists bind specifically to integrin under investigation, reduce cell adhesion and prevent the activation of integrin-mediated intracellular signaling by endogenous agonists.

Molecular Modeling. It is apparent that the large majority of the bioactive compounds in Chart 2 interacts with RGD-binding integrins with nM affinity albeit showing atypical structures as compared to the classic peptide or peptidomimetic ligands. Hence, we performed Molecular Modeling studies to explore the binding modes of representative compounds into integrins whose X-ray structures have been disclosed, namely integrins $\alpha_v\beta_3$ and $\alpha_5\beta_1$. For its high affinity and selectivity, and for the atypical structure lacking the lactam ring, compound **7** was chosen as a model agonist ligand for $\alpha_v\beta_3$ integrin, and the very small β-lactam **6**, lacking the urea group, was selected as a model antagonist for $\alpha_5\beta_1$ integrin.

Docking simulations were performed with Autodock 4.0[30] using the receptor models derived from the deposited X-ray structures, i.e. 4MMX for $\alpha_v\beta_3$ integrin in its extended-active conformation,[31] and 3VI4 for $\alpha_5\beta_1$ integrin in its bent-inactive conformation.[32] The ligand-receptor structures were obtained by a systematic conformer search, followed by geometry optimization. The best-scoring poses are shown in Figure 3 and Figure S1 and S2 (Supporting Information).

Figure 3A shows the carboxylate group of compound **7** closely coordinated to the MIDAS of β_3 subunit, as expected. The ligand shows its urea core in a *S*-shaped *cis,trans* configuration (Figure 3A), which allows to fit the cavity delimited by the residues Tyr122, Arg214, Asn215, Asp217, Ala218, Glu220, Ser121, Ser123 in the β_1 subunit. The receptor keeps in place the carboxylate also by means of three hydrogen bonds, with Tyr122NH (2.09 Å), with Ser123NH (1.55 Å), and with Ser123OH (1.92 Å). In addition, Asn215 contributes to the stabilization of the complex with a hydrogen bond between its carbonyl oxygen and ligand urea NH (2.88 Å). The *o*-tolyl group occupies a hydrophobic cavity delimited by the residues Tyr166, Arg216, Arg214 of the β-subunit (Figure 3A), and by Tyr178 of the α-subunit. Obviously, this short ligand occupies a much smaller portion of the RGD-recognition site of the receptor compared to RGD itself (Figure S1).

The best pose of the ligand **6** involves only residues belonging to the β_1 subunit (Figure 3B and Figure S2 in the Supporting Information). The β-lactam core is framed within a cavity delimited by the residues Ser227, Glu229, Ser134, Tyr133, Asn224. Besides the expected ionic bond between ligand carboxylate and MIDAS (Figure 3B), the carboxylate is stabilized by three hydrogen bonds with the residues Ser134NH (2.99 Å), Asn224NH (1.51 Å), and Asn215CONH (1.60 Å). Finally, the carbonyl oxygen at the C2 position of the β-lactam is hydrogen-bonded to Tyr133NH (2.67 Å). The *o*-tolyl group appears well inserted in a wide cavity establishing interactions with defined residues of the β_1 subunit, i.e. Gly223, Pro186, Cys187, Cys187, and the phenol ring of Tyr133.

DISCUSSION AND CONCLUSIONS

To discuss how the structural changes modified the biological activities, the new compounds were compared with the previously reported β-lactams **A-F** (Chart 1 and 2, and Figure S3).

Compound **1** showed to increase the adhesion of both model cell lines for $\alpha_v\beta_3$ and $\alpha_4\beta_1$ integrins (Table 1 and Figure 1). Competitive binding assays or SPA using isolated receptors confirmed that this compound binds to both integrins with moderate affinity (Table 2). Due to the very small size, it seems plausible that this ligand could interact only with the β-subunits, thanks to the ionic bond between its carboxylate group and the MIDAS. The dual efficacy of **1** would be the result of the minimal structure of **1** lacking of any pharmacophores to specifically address the β_3- or β_1-subunits. Compared to compound **A**, the constraint due to the C=C bond on the ring in **1** had no effect on the affinity for $\alpha_v\beta_3$ but it reversed the functional activity, from antagonism of **A** to agonism of **1**. It is possible that the less flexible ligand **1** could establish better non-covalent interactions with the receptor in the coordination of the Mg^{++} held in the metal-ion dependent adhesion site (MIDAS) of the β_3 subunit.

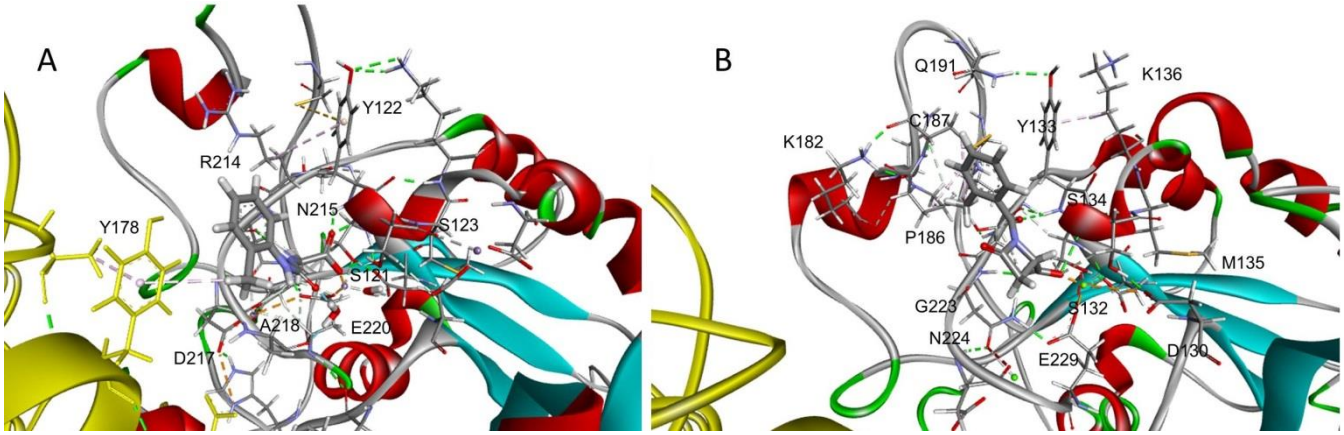

Figure 3. Side views of the calculated binding poses: A) compound **7** into the $\alpha_v\beta_3$ integrin (pdb code 4MMX); B) compound **6** into the $\alpha_5\beta_1$ integrin (pdb code 3VI4). The ligands are rendered in sticks, the protein backbone is represented as a solid ribbon, the α subunit being highlighted in yellow. The relevant receptor residues are rendered in thick lines and indicated by the one-letter code. Dashed green lines represent hydrogen bonds, cation-π interactions are rendered in brown, π–π interactions in pink, hydrophobic interactions in white. Divalent cations are shown as gray spheres.

It could be due to a greater directionality because of the conformational restriction along with the increased acidity of the α,β-unsaturated acid compared to the saturated carboxylic acid in compound **A**. Both these effects could cooperate in the interaction of this small molecule with the β_3 subunit thus promoting an active open-extended integrin conformation leading to the agonism of **1**.[19] As previously demonstrated, in fact, there is an autonomous regulation of integrin conformations by the β_3 subunit that suggests its major role in integrin activation.[33] It could be also observed that the lack of a N-substituent as in compounds **1** and **A** compared to **C**, leads to a shift in integrin selectivity from $\alpha_4\beta_1$ to $\alpha_v\beta_3$, instead. The significance of the two structural elements, COOH and *N*-substituent, was confirmed by the behavior of compound **3**: the lack of the COOH group completely deactivated the ligand towards $\alpha_v\beta_3$ and a poor residual activity for $\alpha_4\beta_1$ remained due to the *N*-*o*-tolyl-group. However, the presence of a COOH is not still sufficient for integrin recognition, as demonstrated by the inactivity of compound **2** that has a longer C4 side chain than **A**. A shorter distance between the C4 carboxylate and the β-lactam could favor a cooperative interaction with the very close ADMIDAS metal site of the β_3 subunit thus enforcing the integrin recognition,[34] not possible in a longer chain as in compound **2**.

A lack of the ureidic NH group as in compound **4** and **6** leads to a deactivation toward $\alpha_4\beta_1$, compared with **C** and **D** that are good $\alpha_4\beta_1$ ligands. In contrast, **4** and especially **6** are selective antagonist toward $\alpha_5\beta_1$. The selectivity switch from $\alpha_4\beta_1$ to $\alpha_5\beta_1$ could be attributed to more favorable interactions with the α_5 subunit due to an increased basicity of the imide group compared to the urea, and with a hydrogen bond acceptor character. The absence of the classical guanidinium group, as in the RGD sequence, would not be crucial to gain recognition by $\alpha_5\beta_1$ or $\alpha_v\beta_3$, as demonstrated by small non-peptidic molecules without the guanidinium group previously developed as selective ligands of integrin $\alpha_5\beta_1$.[35]

The proline derivative **5** with a larger ring than that of β-lactam **D** and without the imide group was a poor ligand for $\alpha_v\beta_3$, but it maintained the activity toward $\alpha_5\beta_1$ and $\alpha_4\beta_1$. Interestingly in this case there is a complete switch in the ligand behavior: from antagonism of the β-lactam **D** to agonism of proline derivative **5**.

The complete absence of a cyclic scaffold, such as in compounds **7** and **8**, had a strong effect on increasing the agonist selectivity toward $\alpha_v\beta_3$ compared to the corresponding cyclic ligands **D** and **C**, which were more active or only active toward $\alpha_4\beta_1$, respectively. In particular, the linear compound **8** and β-lactam **C** turned out to be both agonists but with a switch in selectivity from $\alpha_4\beta_1$ for **C** to $\alpha_v\beta_3$ for **8**. This selectivity of **C** for $\alpha_4\beta_1$ could be tentatively attributed to favorable interactions with the ligand-binding domain αI of the $\alpha_4\beta_1$ integrin,[36-37] which is lost in linear compound **8**. As a general consideration, a linear molecule could be useful to influence the selectivity, but the cyclic β-lactam analog has a higher potency, probably because of better side chain alignment on the receptor due to the cyclic core.

The configuration at the C-4 position of the β-lactam ring turned to be very important. A change from the (*S*) configuration in compounds **D** and **F**, to the (*R*) configuration in compounds **9** and **11** switched off the activity. This stereopreference in integrin recognition is consistent with results that were recently reported.[38] Compound **10** with an (*R*) C-4 configuration interestingly was a selective antagonist of $\alpha_5\beta_1$, whereas its (*S*) enantiomer **E** was a selective ligand for $\alpha_v\beta_3$. In general, it could be observed that (*S*)-enantiomers are preferred for receptor recognition, but (*R*) enantiomers should be carefully evaluated.[38]

Molecular docking computations suggested useful hints to explain the preference of compounds **7** and **6** towards integrins $\alpha_v\beta_3$ and $\alpha_5\beta1$, respectively. In $\alpha_5\beta_1$ integrin, the MIDAS is topped by a large hydrophobic pocket capable to host the *o*-tolyl group of β-lactam **6** (Figure 3B). In contrast, in the $\alpha_v\beta_3$ integrin this hydrophobic cavity is considerably narrowed for the presence of large residues, especially Arg214, Asn215, and Arg216,[39] thus preventing ligand **6** to fit the receptor.

On the other hand, ligand **7**, but not ligand **6**, is capable to skirt these obstacles and to insert its *o*-tolyl moiety into the

large pocket delimited by hydrophobic residues of the α- and β-subunits (Figure 3A), thanks to the comparatively longer and more flexible *S*-shaped urea backbone.

Furthermore, compound **7** was shown to behave as an agonist of $\alpha_v\beta_3$ integrin, despite of the lack of relevant interactions with the α_v-subunit. The docking pose clearly showed that this ligand occupies only a small fraction of the RGD-binding site (Figure S1). Previously, small molecules, such as the thyroid hormone,[40] were shown to bind integrin $\alpha_v\beta_3$ mainly by interacting with the β-subunit. More recent evidence strongly supported that ligand carboxylate binding to the MIDAS can be sufficient to open the headpiece, and hence to activate the integrin, while Arg (or any mimetics) might not be required.[34]

Intriguingly, ligand **6** was shown to act as a pure antagonist of $\alpha_5\beta_1$ integrin. Extensive investigations on $\alpha_{IIb}\beta_3$ and $\alpha_v\beta_3$ integrins showed that the mechanism of extension and activation requires a specific reorganization of pre-existing interaction networks around Y122 of the β-subunit, in the proximity of the ligand recognition site.[41, 31]

In this perspective, the peculiar structure of compound **6** appears perfectly adequate to block the position of Tyr122 in the inactive conformation. Antagonism would be determined by the presence of the bulky, *o*-methylbenzoyl aromatic group that optimally packs against Tyr122, therefore freezing hinge opening and domain traslocation.[31, 42]

In summary, this study contributes to a better comprehension of the structural requirements relevant to confer agonist or antagonist behavior toward integrins, and, moreover, new potent and selective integrin agonists were discovered. In recent decades, many efforts have been made to develop integrin antagonists, whereas integrin agonists have been considered as potential therapeutics only very recently. Agonists for $\alpha_v\beta_3$ could be useful for functionalizing titanium surfaces to foster bone regeneration on implant materials.[22] In addition, agonists for $\alpha_4\beta_1$ have been proposed to enhance stem cell therapy when coadministered with progenitor cells by increasing cell adhesion,[43] or enhance vascularization in regenerative medicine.[44]

EXPERIMENTAL SECTION

General methods. Compounds **1**, **13**, **15**, and **26** were synthesized according to our previously reported procedures.[14, 17] Compounds **17** and **21** are known and were synthesized according to reported procedures.[18-20] Structure and purity of known compounds was assessed by ^{1}H NMR and HPLC-MS analysis: spectroscopic data are in accordance to those reported in literature. Target compounds were determined to be ≥ 95% pure by analytical HPLC analyses (Supporting information). Optical purity of compounds synthetized from D-aspartic acid was assessed by chiral-HPLC analysis on compound **22** chosen as a model using a Chiralpack IA column, eluent: isopropanol/n-hexane 50:50, flow= 0.5 mL/min, temperature = 40°C.

General procedure for N-acylation (GP1) In a 25 mL two neck flask the starting compound (1 equiv) was dissolved in anhydrous CH_2Cl_2 (11 mL/mmol) under a nitrogen atmosphere. Anhydrous TEA was added dropwise, followed by a dropwise addition of the commercially available o-tolylisocyanate. The mixture was stirred at room temperature until a complete consumption of the starting beta-lactam (4h, TLC monitoring) and then quenched with a saturated aqueous solution of NH_4Cl. The mixture was then extracted with CH_2Cl_2 (3 x 10mL), the organic layers were collected, dried over anhydrous Na_2SO_4, concentrated in vacuum and purified by flash-chromatography affording the desired N-acylated compounds.

General procedure for hydrogenolysis (GP2). In a 25 mL two-neck flask the starting benzyl ester (1 equiv) was dissolved in a 1:1 mixture of THF and CH_3OH (22 mL/mmol) and Pd/C (10% w/w) was added. The solution was then stirred under a H_2 atmosphere (1 atm) at room temperature. After a complete consumption of the starting material (TLC monitoring, 2h) the reaction mixture was filtered through celite and concentrated in vacuum. The crude was then triturated with few drops of pentane to afford the desired carboxylic acids.

2-(4-Oxoazetidin-2-yl)acetyl)glycine (**2**). Following GP2, compound **16** (68 mg, 0.25 mmol) yielded compound **2** as a waxy solid (42 mg, 91%). ^{1}H NMR (400 MHz, CD_3OD) δ (ppm) 3.98 – 3.94 (m, 1H), 3.93 (d, *J* = 18.0, 1H), 3.89 (d, *J* = 18.0 Hz, 1H), 3.10 (dd, *J* = 15.0, 4.9 Hz, 1H), 2.69 (dd, *J* = 15.0, 1.9 Hz, 1H), 2.66 – 2.55 (m, 2H); ^{13}C NMR (100 MHz, CD_3OD) δ (ppm) 173.23, 173.21, 170.4, 45.9, 43.6, 42.1, 41.8; IR (film, cm^{-1}) 3316, 2927, 1730, 1636, 1534, 1476, 1414, 1379, 1193.

2-Oxo-*N*-(*o*-tolyl)azetidine-1-carboxamide (**3**). In a 25 mL two-neck flask, a solution of sodium bis(trimethylsilyl)amide(NaHMDSA) (1.0 M in THF, 875 µL, 1.25 equiv) was added dropwise to a solution of 2-azetidinone (50 mg, 0.7 mmol, 1 equiv) in anhydrous THF (6.2 mL) at −78 °C under a nitrogen atmosphere. The mixture was stirred for 15 min, then o-tolylisocyanate (108 µL, 0.875 mmol, 1.25 equiv) was added dropwise. After completion (TLC monitoring, 30 min), the mixture was quenched with a saturated aqueous solution of NH_4Cl and extracted with CH_2Cl_2 (3 × 10 mL). The combined organic extracts were dried over anhydrous Na_2SO_4, concentrated in vacuum, and purified by flash chromatography (cyclohexane/AcOEt 3:2), affording **3** as a colorless oil (60 mg, 42%). ^{1}H NMR (400 MHz, $CDCl_3$) δ (ppm) 8.44 (bs, 1H), 7.95 (d, *J* = 8.0 Hz, 1H), 7.23 – 7.17 (m, 2H), 7.04 (t, *J* = 7.4 Hz, 1H), 3.72 (t, *J* = 4.8 Hz, 2H), 3.12 (t, *J* = 4.8 Hz, 2H), 2.30 (s, 3H); ^{13}C NMR (100 MHz, $CDCl_3$) δ (ppm) 167.4, 147.9, 135.3, 130.3, 127.4, 126.7, 124.3, 121.0, 37.3, 36.0, 17.6; HPLC-MS (ESI$^+$) Rt= 6.8 min, m/z=205 [M+H]$^+$; IR (film, cm^{-1}) 3298, 2919, 1762, 1710, 1614, 1552, 1459, 1314, 1297, 1191

2-(1-(2-Methylbenzoyl)-4-oxoazetidin-2-yl)acetic acid (**4**). Following GP2, compound **14** (32 mg, 0.09 mmol) yielded compound **4** as a waxy solid (22 mg, 99%). ^{1}H NMR (400 MHz, CD_3OD) δ (ppm) 7.45 (d, *J* = 7.7 Hz, 1H), 7.39 (t, *J* = 7.5 Hz, 1H), 7.24 (dd, *J* = 14.4, 7.3 Hz, 2H), 4.47 (ddd, *J* = 10.2, 7.6, 3.6 Hz, 1H), 3.30 (dd, *J* = 16.1, 6.4 Hz, 1H), 3.13 (dd, *J* = 16.3, 3.7 Hz, 1H), 3.01 (dd, *J* = 16.3, 3.7 Hz, 1H), 2.85 (dd, *J* = 16.3, 8.3 Hz, 1H), 2.38 (s, 3H); ^{13}C NMR (100 MHz, CD_3OD) δ (ppm) 174.0, 168.7, 165.6, 137.7, 135.0, 132.0, 131.6, 129.4, 126.5, 48.6, 43.0, 37.2, 19.5; HPLC-MS (ESI$^+$) Rt=5.1 min, m/z=248 [M+H]$^+$; IR (film, cm^{-1}) 2960, 2857, 1795, 1704, 1677, 1430, 1327, 1224, 1184

(*o*-Tolylcarbamoyl)-L-proline (**5**). Following GP2, compound **18** (60 mg, 0.18 mmol) yielded compound **5** as a waxy

solid (44 mg, 99%). ^{1}H NMR (400 MHz, CD_3OD) δ (ppm) 7.38 (d, *J* = 7.8 Hz, 1H), 7.17 (d, *J* = 7.5 Hz, 1H), 7.12 (t, *J* = 7.4 Hz, 1H), 7.02 (t, *J* = 7.3 Hz, 1H), 4.31 (t, *J* = 5.9 Hz, 1H), 3.61 – 3.56 (m, 2H), 2.27 (s, 3H), 2.17 – 1.91 (m, 4H); ^{13}C NMR (100 MHz, CD_3OD) δ (ppm) 177.0, 157.6, 138.1, 134.9, 131.3, 127.5, 127.1, 126.6, 60.8, 47.5, 31.0, 25.4, 18.2; HPLC-MS (ESI^+) Rt= 3.3 min, m/z=249 $[M+H]^+$; IR (film, cm^{-1}) 3423, 2927, 1720, 1709, 1639, 1527, 1457, 1377, 1254, 1199, 1124; $[\alpha]^D_{20}$ = - 46.6 (c=10.0 mg/mL, CH_3OH)

(*S*)-1-(2-Methylbenzoyl)-4-oxoazetidine-2-carboxylic acid (**6**). Following GP2, compound **12** (80 mg, 0.25 mmol) yielded compound **6** as a waxy solid (53 mg, 91%). ^{1}H NMR (400 MHz, CD_3OD) δ (ppm) 7.49 (d, *J* = 7.7 Hz, 1H), 7.39 (t, *J* = 7.5 Hz, 1H), 7.27 – 7.21 (m, 2H), 4.59 (dd, *J* = 7.0, 3.4 Hz, 1H), 3.41 (dd, *J* = 16.1, 7.0 Hz, 1H), 3.05 (dd, *J* = 16.1, 3.4 Hz, 1H), 2.40 (s, 3H); ^{13}C NMR (100 MHz, CD_3OD) δ (ppm) 172.9, 167.7, 164.0, 138.1, 134.4, 132.2, 131.7, 129.4, 126.5, 50.4, 41.5, 19.5; HPLC-MS (ESI^+) Rt= 6.3 min, m/z=234 $[M+H]^+$; IR (film, cm^{-1}) 2967, 2930, 1806, 1728, 1686, 1603, 1324, 1259, 1184; $[\alpha]^D_{20}$ = - 80.7 (c= 10 mg/mL, CH_2Cl_2)

(*o*-Tolylcarbamoyl)-glycine (**7**). Following GP2, compound **19** (70 mg, 0.23 mmol) yielded compound **7** as a waxy solid (47 mg, 97%). ^{1}H NMR (400 MHz, CD_3OD) δ (ppm) 7.50 (d, *J* = 7.9 Hz, 1H), 7.18 – 7.11 (m,, 2H), 7.01 (t, *J* = 7.4 Hz, 1H), 3.92 (s, 2H), 2.26 (s, 3H); ^{13}C NMR (100 MHz, CD_3CN) δ (ppm) 172.8, 157.2, 136.6, 130.4, 130.0, 126.0, 124.0, 123.5, 35.3, 16.6; HPLC-MS (ESI^+) Rt= 2.5 min, m/z=209 $[M+H]^+$; IR (film, cm^{-1}) 3411, 3263, 2988, 1707, 1614, 1598, 1459, 1390, 1239, 1114.

3-(3-(*o*-Tolyl)ureido)propanoic acid (**8).** Following GP2, compound **20** (45 mg, 0.14 mmol) yielded compound **8** as a waxy solid (30 mg, 99%). ^{1}H NMR (400 MHz, CD_3OD) δ (ppm) 7.48 (d, *J* = 7.9 Hz, 1H), 7.16 – 7.11 (m, 2H), 7.00 (t, *J* = 7.8 Hz, 1H), 3.45 (t, *J* = 6.3 Hz, 2H), 2.53 (t, *J* = 6.3 Hz, 2H), 2.23 (s, 3H); ^{13}C NMR (100 MHz, CD_3OD) δ (ppm) 175.8, 158.8, 138.1, 131.9, 131.4, 127.4, 125.4, 125.0, 36.8, 35.6, 18.0; HPLC-MS (ESI^+) Rt= 2.6 min, m/z=223 $[M+H]^+$; IR (film, cm^{-1}) 3303, 3032, 2954, 1715, 1632, 1573, 1418, 1296, 1222, 1106.

(*R*)-4-Oxo-1-(o-tolylcarbamoyl)azetidine-2-carbo xylic acid (**9).** Following GP2, compound **22** (105 mg, 0.31 mmol) yielded compound **9** as a white solid (74 mg, 97%). ^{1}H NMR (400 MHz, $CDCl_3$) δ (ppm) 8.37 (bs, 1H), 8.19 (bs, 1H), 7.86 (d, *J* = 8.4 Hz, 1H), 7.18 – 7.15 (m, 2H), 7.05 (t, *J* = 7.4 Hz, 1H), 4.59 (dd, *J* = 6.2, 2.2 Hz, 1H), 3.37 (dd, *J* = 16.0, 6.2 Hz, 1H), 3.20 (dd, *J* = 16.0, 2.2 Hz, 1H), 2.28 (s, 3H); ^{13}C NMR (100 MHz, $CDCl_3$) δ (ppm) 172.0, 165.7, 147.9, 134.6, 130.5, 128.0, 126.8, 125.1, 121.5, 49.7, 41.3, 17.6; HPLC-MS (ESI^+) Rt=5.9 min, m/z=249 $[M+H]^+$; IR (film, cm^{-1}) 3344, 3024, 2966, 2962, 1775, 1717, 1615, 1593, 1459, 1308, 1252; m.p. 121-123 °C; $[\alpha]^D_{20}$ = +114.3 (c=11.5 mg/mL, CH_2Cl_2)

(*R*)-3-(4-oxo-1-(*o*-tolylcarbamoyl)azetidine-2-car boxamido)propanoic acid (**10**). Following GP2, compound **23** (46 mg, 0.11 mmol) yielded compound **10** as a waxy solid (34 mg, 97%). ^{1}H NMR (400 MHz, $CDCl_3$) δ (ppm) 8.46 (bs, 1H), 7.83 – 7.81 (m, 2H), 7.21 – 7.18 (m, 2H), 7.07 (t, *J* = 7.4 Hz, 1H), 4.59 (dd, *J* = 6.0, 3.1 Hz, 1H), 3.63 – 3.52 (m, 2H), 3.44 (dd, *J* = 16.2, 3.1 Hz, 1H), 3.24 (dd, *J* = 16.2, 6.0 Hz, 1H), 2.59 (t, *J* = 5.6 Hz, 2H), 2.29 (s, 3H); ^{13}C NMR (100 MHz, CD_3OD) δ (ppm) 175.3, 171.0, 168.0, 149.4, 136.4, 131.5, 129.9, 127.6, 126.0, 123.0, 51.6, 42.1, 36.7, 34.5, 17.7; HPLC-MS (ESI^+) Rt=4.3 min, m/z=320 $[M+H]^+$, 342 $[M+Na]^+$; IR (film, cm^{-1}) 3352, 1779, 1734, 1708, 1648, 1595, 1550, 1458, 1311, 1254, 1203; $[\alpha]^D_{20}$ = +56.7 (c=7.0 mg/mL, CH_3OH)

(*R*)-(4-(2-carboxy-4-oxoazetidine-1-carboxamido) phenyl)methanaminium 2,2,2-trifluoroacetate (**11**). In a 25 mL two-neck flask, compound **25** (72 mg, 0.19 mmol, 1 equiv) was dissolved in CH_2Cl_2 (3.5 mL) under a nitrogen atmosphere and trifluoroacetic acid (TFA) was added dropwise at 0°C. New TFA aliquots were added each 30 mins at 0°C until a complete conversion (261 µL, 3.42 mmol, 18 equiv in total, 8 h, TLC monitoring). The solvent was removed under reduced pressure and the crude was triturated with few drops of pentane, yielding compound **11** (67 mg, 94%) as a waxy solid. ^{1}H NMR (400 MHz, CD_3OD) δ (ppm) 7.57 (d, *J* = 8.4 Hz, 2H), 7.41 (d, *J* = 8.4 Hz, 2H), 4.61 – 4.59 (m, 1H), 4.08 – 4.06 (m, 2H), 3.50 (dd, *J* = 15.7, 5.6 Hz, 1H), 3.12 (d, *J* = 15.7 Hz, 1H); ^{13}C NMR (100 MHz, CD_3OD) δ (ppm) 171.9, 167.1, 148.8, 139.4, 130.9, 130.2, 121.5, 43.8, 43.6, 42.1; ^{19}F NMR (375 MHz, CD_3OD) δ (ppm) -76.7 ppm; HPLC-MS (ESI^+) Rt=1.3 min, m/z=247 $[M+H]^+$; IR (film, cm^{-1}) 3417, 3301, 2969, 1781, 1743, 1708, 1666, 1604, 1549, 1421, 1320, 1184; $[\alpha]^D_{20}$ = +96.4 (c=11.3 mg/mL, CH_3OH).

Benzyl (*S*)-1-(2-methylbenzoyl)-4-oxoazetidine-2-carboxylate (**12**). In a 10 mL two-neck flask, the commercially available benzyl (*S*)-4-oxoazetidine-2-carboxylate (62 mg, 0.3 mmol, 1 equiv) was dissolved in anhydrous CH_2Cl_2 (1.5 mL) under nitrogen. TEA (135 µL, 0.96 mmol, 3.2 equiv) and DMAP (4 mg, 0.03 mmol, 0.1 equiv) were then added. O-toluylchloride (78 µL, 0.6 mmol, 2 equiv) was then added dropwise at 0°C. After 10 minutes, the solution was warmed to rt and left under stirring. After complete consumption of the starting material (6 h), the mixture was quenched with a saturated aqueous solution of NH_4Cl and extracted with CH_2Cl_2 (3 × 10 mL). The combined organic extracts were dried over anhydrous Na_2SO_4, concentrated in vacuum, and purified by flash chromatography (cyclohexane/AcOEt 7:3), affording **12** as a colorless oil (83 mg, 86%). ^{1}H NMR (400 MHz, $CDCl_3$) δ (ppm) 7.52 (d, *J* = 7.5 Hz, 1H), 7.44 – 7.35 (m, 6H), 7.26 (t, *J* = 7.2 Hz, 2H), 5.30 (d, J_{AB} = 12.2 Hz, 1H), 5.26 (d, J_{AB} = 12.1 Hz, 1H), 4.68 (dd, *J* = 6.8, 3.5 Hz, 1H), 3.34 (dd, *J* = 16.1, 6.8 Hz, 1H), 3.07 (dd, *J* = 16.1, 3.5 Hz, 1H), 2.41 (s, 3H); ^{13}C NMR (100 MHz, $CDCl_3$) δ (ppm) 169.0, 165.8, 161.3, 137.4, 134.7, 132.1, 131.6, 130.8, 128.7, 128.64, 128.57, 128.4, 125.4, 67.7, 48.7, 40.4, 19.5; HPLC-MS (ESI^+) Rt= 10.2 min, m/z=324 $[M+H]^+$; IR (film, cm^{-1}) 3031, 2962, 2928, 1805, 1746, 1684, 1490, 1386, 1288, 1207, 1145; $[\alpha]^D_{20}$ = - 78.2 (c=11.6 mg/mL, CH_2Cl_2)

Benzyl 2-(1-(2-methylbenzoyl)-4-oxoazetidin-2-yl) acetate (**14**). In a 10 mL two-neck flask, compound **13** (50 mg, 0.23 mmol, 1 equiv) was dissolved in anhydrous CH_2Cl_2 (1.2 mL) under nitrogen. TEA (103 µL, 0.73 mmol, 3.2 equiv) and DMAP (3 mg, 0.023 mmol, 0.1 equiv) were then added. O-toluylchloride (60 µL, 0.46 mmol, 2 equiv) was then added dropwise at 0°C. After 10 minutes, the solution was warmed to rt and left under stirring overnight. After 18 h, the mixture was quenched with a saturated aqueous solution of NH_4Cl and extracted with CH_2Cl_2 (3 × 10 mL). The combined organic extracts were dried over anhydrous Na_2SO_4, concentrated in vacuum, and purified by flash chromatography (cyclohex-

ane/AcOEt 7:3), affording **14** as a colorless oil (60 mg, 77%). ^{1}H NMR (400 MHz, $CDCl_3$) δ (ppm) 7.44 – 7.32 (m, 7H), 7.25 – 7.22 (m, 2H), 5.19 (d, J_{AB} = 12.3 Hz, 1H), 5.15 (d, J_{AB} = 12.2 Hz, 1H), 4.56 – 4.50 (m, 1H), 3.37 – 3.25 (m, 2H), 2.94 (dd, *J* = 16.6, 3.6 Hz, 1H), 2.85 (dd, *J* = 16.3, 8.4 Hz, 1H), 2.40 (s, 3H); ^{13}C NMR (100 MHz, $CDCl_3$) δ (ppm) 169.7, 166.8, 163.0, 137.0, 135.3, 132.7, 131.3, 130.8, 128.6, 128.58, 128.45, 128.36, 125.4, 66.8, 46.6, 42.1, 36.8, 19.6; HPLC-MS (ESI^+) Rt=7.6 min, m/z=338 $[M+H]^+$; IR (film, cm^{-1}) 2958, 2929, 1796, 1734, 1676, 1511, 1456, 1289, 1184.

Benzyl (2-(4-oxoazetidin-2-yl)acetyl)glycinate (**16**). In a 25 mL two-neck flask, compound **15** (76 mg, 0.59 mmol, 1 equiv) was dissolved in a mixture of CH_2Cl_2 (6.6 mL) and CH_3CN (1.3 mL) under nitrogen. Dicyclohexylcarbodiimide (DCC) (16 mg, 0.79 mmol, 1.1 equiv) was then added at 0°C. It was followed by the dropwise addition of a previously prepared solution of glycine benzylester p-chlorohydrate salt (179 mg, 0.89 mmol, 1.5 equiv) and TEA (132 µL, 0.94 mmol, 1.6 equiv) in CH_2Cl_2 (7.4 mL). After addition of catalytic DMAP (14 mg, 0.12 mmol, 0.2 equiv), the solution was warmed to rt and left under stirring overnight. After complete consumption of the starting material (16 h), the mixture was quenched with H_2O and extracted with CH_2Cl_2 (3 × 10 mL). The collected organic layers were dried on anhydrous Na_2SO_4 and filtered. The crude was suspended in AcOEt, and the solid residual dicyclohexylurea was eliminated by filtration. The organic layer was concentrated in vacuum and purified by flash chromatography (CH_2Cl_2/AcOEt from 3:2 to 100% AcOEt), yielding compound **16** (68 mg, 91%) as a colorless oil. ^{1}H NMR (400 MHz, $CDCl_3$) δ (ppm) 7.37 – 7.31 (m, 5H), 6.99 (bs, 1H), 6.72 (bs, 1H), 5.16 (d, *J* = 12.3 Hz, 1H), 5.12 (d, *J* = 12.3 Hz, 1H), 4.15 (dd, *J* = 18.1, 6.1 Hz, 1H), 3.97 – 3.95 (m, 1H), 3.91 (dd, *J* = 18.1, 5.0 Hz, 1H), 3.09 (dd, *J* = 14.8, 3.2 Hz, 1H), 2.68 – 2.55 (m, 2H), 2.45 (dd, *J* = 14.4, 9.4 Hz, 1H); ^{13}C NMR (100 MHz, $CDCl_3$) δ (ppm) 170.7, 170.1, 167.5, 134.9, 128.6, 128.5, 128.3, 67.2, 44.8, 43.3, 41.5, 41.1; HPLC-MS (ESI^+) Rt=10.5 min, m/z=277 $[M+H]^+$, 294 $[M+H_2O]^+$; IR (film, cm^{-1}) 3300, 2954, 1742, 1657, 1562, 1411, 1192, 1126.

Benzyl (o-tolylcarbamoyl)-L-prolinate (**18**). Compound **17** (82 mg, 0.26 mmol, 1 equiv) was treated with TEA (73 µL, 0.52 mmol, 2 equiv) and o-tolylisocyanate (36 µL, 0.29 mmol, 1.1 equiv) following GP1. Chromatography (cyclohexane/AcOEt 1:1) yielded **18** as a colorless oil (63 mg, 72%). ^{1}H NMR (400 MHz, $CDCl_3$) δ (ppm) 7.73 (d, *J* = 8.0 Hz, 1H), 7.36 – 7.29 (m, 5H), 7.18 – 7.12 (m, 2H), 6.99 (t, *J* = 7.4 Hz, 1H), 6.34 (bs, 1H), 5.22 (d, J_{AB} = 12.4 Hz, 1H), 5.14 (d, J_{AB} = 12.4 Hz, 1H), 4.55 (dd, *J* = 8.1, 2.3 Hz, 1H), 3.61 – 3.48 (m, 2H), 2.20 (s, 3H), 2.16 – 1.99 (m, 4H); ^{13}C NMR (100 MHz, $CDCl_3$) δ (ppm) 172.6, 154.1, 136.7, 135.5, 130.1, 128.4, 128.24, 128.16, 128.0, 126.5, 123.7, 122.4, 66.8, 59.3, 46.1, 29.6, 24.4, 17.6; HPLC-MS (ESI^+) Rt= 9.4 min, m/z=338 $[M+H]^+$; IR (film, cm^{-1}) 3313, 2971, 1743, 1640, 1524, 1455, 1369, 1254, 1169; $[\alpha]^D_{20}$ = - 55.5 (c=11.0 mg/mL, CH_2Cl_2).

Benzyl 3-(3-(o-tolyl)ureido)propanoate (**20**). Commercially available beta alanine benzylester *p*-toluenesulfonate salt (70 mg, 0.2 mmol, 1 equiv) was treated with TEA (56 µL, 0.4mmol, 2 equiv) and o-tolylisocyanate (27 µL, 0.22 mmol, 1.1 equiv) following GP1. Chromatography (cyclohexane/AcOEt 3:2) yielded **20** as a colorless oil (47 mg, 76%). ^{1}H NMR (400 MHz, CD_3CN) δ (ppm) 7.63 (d, *J* = 8.0 Hz, 1H), 7.37 – 7.31 (m, 5H), 7.16 – 7.10 (m, 2H), 6.96 (t, *J* = 7.0 Hz, 1H), 6.79 (bs, 1H), 5.68 (bs, 1H), 5.11 (s, 2H), 3.43 (q, *J* = 6.4 Hz, 2H), 2.56 (t, *J* = 6.4 Hz, 2H), 2.25 (s, 3H); ^{13}C NMR (100 MHz, CD_3CN) δ (ppm) 173.0, 156.7, 138.5, 137.4, 131.2, 130.2, 129.5, 129.04, 128.95, 127.2, 124.4, 123.6, 66.9, 36.6, 35.7, 18.2; HPLC-MS (ESI^+) Rt= 8.4 min, m/z=313 $[M+H]^+$; IR (film, cm^{-1}) 3308, 3066, 2954, 1727, 1632, 1566, 1456, 1419, 1253, 1186.

Benzyl (*R*)-4-oxo-1-(o-tolylcarbamoyl)azetidine-2-carboxylate (**22**). Compound **21** (80 mg, 0.39 mmol, 1 equiv) was treated with TEA (66 µL, 0.47 mmol, 1.2 equiv) and o-tolylisocyanate (58 µL, 0.47 mmol, 1.2 equiv) following GP1. Chromatography (CH_2Cl_2/Et_2O 95:5) yielded **22** as a waxy solid (112 mg, 85%). ^{1}H NMR (400 MHz, $CDCl_3$) δ (ppm) 8.29 (bs, 1H), 7.93 (d, *J* = 8.0 Hz, 1H), 7.41 – 7.31 (m, 5H), 7.25 – 7.15 (m, 2H), 7.07 (t, *J* = 7.4 Hz, 1H), 5.30 (d, JAB = 12.2 Hz, 1H), 5.25 (d, JAB = 12.2 Hz, 1H), 4.62 (dd, *J* = 6.2, 2.9 Hz, 1H), 3.40 (dd, *J* = 15.8, 6.2 Hz, 1H), 3.11 (dd, *J* = 15.8, 2.9 Hz, 1H), 2.31 (s, 3H); ^{13}C NMR (100 MHz, $CDCl_3$) δ (ppm) 168.8, 165.2, 146.8, 135.0, 134.7, 130.4, 128.65, 128.61, 128.3, 127.7, 126.8, 124.7, 121.2, 67.8, 48.9, 41.2, 17.6; HPLC-MS (ESI^+) Rt=10.5 min, m/z=339 $[M+H]^+$; IR (film, cm^{-1}) 3346, 3031, 2924, 1776, 1751, 1718, 1614, 1593, 1387, 1252, 1187; $[\alpha]^D_{20}$ = + 96.4 (c=10.0 mg/mL, CH_2Cl_2).

Benzyl (R)-3-(4-oxo-1-(o-tolylcarbamoyl)azetidine -2-carboxamido)propanoate (**23**). In a 25 mL two-neck flask, compound **9** (69 mg, 0.28 mmol, 1 equiv) was dissolved in anhydrous CH_2Cl_2 (2.8 mL) under nitrogen. Oxalyl chloride (29 µL, 0.34 mmol, 1.2 equiv) was then added dropwise. The mixture was left under stirring for 30 minutes, then beta alanine benzylester *p*-toluenesulfonate salt (98 mg, 0.28 mmol, 1 equiv) was added, followed by the dropwise addition of TEA (157 µL, 1.12 mmol, 4 equiv) at 0°C and DMAP (7 mg, 0.056 mmol, 0.2 equiv). After 10 minutes, the solution was warmed to rt and left under stirring overnight. After complete consumption of the starting material (16 h), the mixture was quenched with a saturated aqueous solution of NH_4Cl and extracted with CH_2Cl_2 (3 × 10 mL). The combined organic extracts were dried over anhydrous Na_2SO_4, concentrated in vacuum, and purified by flash chromatography (cyclohexane/AcOEt 3:2), affording **23** as a colorless oil (56 mg, 50%). ^{1}H NMR (400 MHz, $CDCl_3$) δ (ppm) 8.46 (bs, 1H), 7.89 (d, *J* = 8.4 Hz, 1H), 7.73 (bs, 1H), 7.35 – 7.29 (m, 5H), 7.22 – 7.18 (m, 2H), 7.07 (t, *J* = 7.4 Hz, 1H), 5.11 (s, 2H), 4.54 (dd, *J* = 6.1, 3.1 Hz, 1H), 3.66 – 3.54 (m, 2H), 3.46 (dd, *J* = 16.3, 3.1 Hz, 1H), 3.26 (dd, *J* = 16.3, 6.1 Hz, 1H), 2.63 (t, *J* = 6.2 Hz, 2H), 2.30 (s, 3H); ^{13}C NMR (100 MHz, $CDCl_3$) δ (ppm) 171.6, 167.5, 166.8, 148.6, 135.5, 134.7, 130.5, 128.5, 128.22, 128.16, 128.0, 126.7, 124.9, 121.4, 66.5, 51.7, 40.3, 35.3, 33.9, 17.6; HPLC-MS (ESI^+) Rt=9.2 min, m/z=410 $[M+H]^+$; IR (film, cm^{-1}) 3339, 2957, 1773, 1730, 1678, 1615, 1593, 1459, 1253, 1174; $[\alpha]^D_{20}$ = +101.8 (c=9.2 mg/mL, CH_2Cl_2).

Benzyl (R)-1-((4-(((tert-butoxycarbonyl)amino) methyl)phenyl)carbamoyl)-4-oxoazetidine-2-carboxy late (**24**). In a 25 mL two-neck flask, compound **21** (70 mg, 0.34 mmol, 1 equiv) was dissolved in anhydrous CH_2Cl_2 (3.2 mL) under nitrogen. TEA (84 µL, 0.60 mmol, 1.5 equiv) was then added dropwise. The mixture was stirred for 15 minutes, then a solution of freshly prepared isocyanate 26 (1.5 equiv) in anhydrous CH_2Cl_2 (1.6 mL) was added dropwise. The mixture was stirred

at room temperature until a complete consumption of the starting beta-lactam (4h, TLC monitoring) and then quenched with a saturated aqueous solution of NH_4Cl. The mixture was extracted with CH_2Cl_2 (3 x 10mL), the organic layers were collected, dried over anhydrous Na_2SO_4, concentrated in vacuum and purified by flash chromatography (cyclohexane/AcOEt 1:1), affording **24** as a colorless oil (110 mg, 60%). ^{1}H NMR (400 MHz, $CDCl_3$) δ (ppm) 8.27 (bs, 1H), 7.42 (d, *J* = 8.4 Hz, 2H), 7.33 – 7.28 (m, 5H), 7.23 (d, *J* = 8.4 Hz, 2H), 5.28 (d, J_{AB} = 12.2 Hz, 1H), 5.23 (d, J_{AB} = 12.2 Hz, 1H), 4.86 (bs, 1H), 4.59 (dd, *J* = 6.2, 2.9 Hz, 1H), 4.27 – 4.25 (m, 2H), 3.38 (dd, *J* = 15.8, 6.2 Hz, 1H), 3.08 (dd, *J* = 15.8, 2.9 Hz, 1H), 1.45 (s, 9H); ^{13}C NMR (400 MHz, $CDCl_3$) δ (ppm) 168.8, 165.0, 155.8, 146.6, 135.8, 135.1, 134.7, 128.64, 128.62, 128.3, 128.2, 119.9, 79.4, 67.8, 48.9, 44.1, 41.2, 28.4; HPLC-MS (ESI^+) Rt=10.4 min, m/z=471 $[M+H]^+$; IR (film, cm^{-1}) 3344, 2975, 1777, 1751, 1708, 1603, 1542, 1317, 1244, 1170; $[\alpha]^D_{20}$ = +62.2 (c=8.3 mg/mL, CH_2Cl_2)

(*R*)-1-((4-(((tert-butoxycarbonyl)amino)methyl) phenyl)carbamoyl)-4-oxoazetidine-2-carboxylic acid (**25**). Following GP2, compound **24** (110 mg, 0.24 mmol) yielded compound **25** as a waxy solid (78 mg, 88%). ^{1}H NMR (400 MHz, CD_3OD) δ (ppm) 7.43 (d, *J* = 8.4 Hz, 2H), 7.23 (d, *J* = 8.4 Hz, 2H), 4.51 (dd, *J* = 6.4, 2.9 Hz, 1H), 4.19 – 4.17 (m, 2H), 3.45 (dd, *J* = 15.8, 6.4 Hz, 1H), 3.08 (dd, *J* = 15.8, 2.9 Hz, 1H), 1.45 (s, 9H); ^{13}C NMR (100 MHz, CD_3OD) δ (ppm) 173.3, 167.3, 158.4, 149.0, 137.2, 137.0, 128.8, 121.2, 80.2, 50.8, 44.5, 42.1, 28.8; HPLC-MS (ESI^+) Rt=7.1 min, m/z=381 $[M+H_2O]^+$, 386 $[M+Na]^+$; IR (film, cm^{-1}) 3341, 2978, 2932, 1776, 1707, 1604, 1544, 1417, 1321, 1244, 1167; $[\alpha]^D_{20}$ = +44.9 (c=10.0 mg/mL, CH_2Cl_2)

ASSOCIATED CONTENT

Supporting Information. ^{1}H and ^{13}C NMR spectra of compounds **1-25**. Assays procedures and methods. Additional pharmacological assays. Molecular modelling and HPLC traces.

AUTHOR INFORMATION

Corresponding Author

*D.G.: e-mail, daria.giacomini@unibo.it.
*S.S. : e-mail, santi.spampinato@unibo.it

Author Contributions

The manuscript was written through contributions of all authors. All authors have given approval to the final version of the manuscript. ⁼G.M. and M.B. contributed equally.

Funding Sources

This research was supported by University of Bologna (RFO2017 and RFO2018), FARB (FFBO 125290), Fondazione Cassa di Risparmio in Bologna (2018/0347) and Ministero dell'Università e della Ricerca (PRIN2015 project 20157WW5EH).

ACKNOWLEDGMENT

DG would like to thank Mr. Riccardo Pedrazzani for his technical assistance. ACS Authoring Service is acknowledged for the English revision of the manuscript.

ABBREVIATIONS

THF, tetrahydrofuran; TEA, triethylamine; TLC, thin layer chromatography; FN, fibronectin; VCAM-1, vascular cell adhesion molecule-1; SPA, scintillation proximity-binding assay; ERK1/2, extracellular signal-regulated kinases 1 and 2.

REFERENCES

(1) Barczyk, M.; Carracedo, S.; Gullberg, D. Integrins. *Cell Tissue Res.* **2010**, *339*, 269-280.
(2) Hynes, R. O. Integrins: bidirectional, allosteric signaling machines. *Cell* **2002**, *110*, 673-687.
(3) Kuriri, F. A; O'Malley, C. J.; Jackson, D. E. Molecular mechanisms of immunoreceptors in platelets. *Thromb. Res.* **2019**, *176*, 108-114.
(4) Rose, D. M.; Han, J.; Ginsberg, M. H. Alpha4 integrins and the immune response. *Immunol. Rev.* **2002**, *186*, 118–124.
(5) Hamidi, H.; Ivaska, J. Every step of the way: integrins in cancer progression and metastasis. *Nat. Rev. Cancer* **2018**, *18*, 532-547.
(6) Nieberler, M.; Reuning, U.; Reichart, F.; Notni, J.; Wester, H.-J.; Schwaiger, M.; Weinmüller, M.; Räder, A.; Steiger K.; Kessler, H. Exploring the role of RGD-recognizing integrins in cancer. *Cancers* **2017**, *9*, 116.
(7) Humphries, J. D.; Byron, A.; Humphries, M. J. Integrin ligands at a glance. *J. Cell Sci.* **2006**, *119*, 3901-3903.
(8) Luo, B. H.; Springer, T. A. Integrin structures and conformational signaling. *Curr. Opin. Cell Biol.* **2006**, *18*, 579-586.
(9) Moore, T. I.; Aaron, J.; Chew, T.-L.; Springer, T. A. Measuring integrin conformational change on the cell surface with super-resolution microscopy. *Cell Rep.* **2018**, *22*, 1903-1912.
(10) Pandolfi, F.; Franza, L.; Altamura, S.; Mandolini, C.; Cianci, R.; Ansari, A.; Kurnick, J. T. Integrins: integrating the biology and therapy of cell-cell interactions. *Clin. Ther.* **2017**, *39*, 2420-2436.
(11) Ley, K.; Rivera-Nieves, J.; Sandborn, W. J.; Shattil, S. Integrin-based therapeutics: biological basis, clinical use and new drugs. *Nat. Rev. Drug Discov.* **2016**, *15*, 173-183.
(12) Tolomelli, A.; Galletti, P.; Baiula, M.; Giacomini, D. Can integrin agonists have cards to play against cancer? A literature survey of small molecules integrin activators. *Cancers* **2017**, *9*, 78.
(13) Humphries, M. J. Integrin cell adhesion receptors and the concept of agonism. *Trends Pharmacol. Sci.* **2000**, *21*, 29-32.
(14) Galletti, P.; Soldati, R.; Pori, M.; Durso, M.; Tolomelli, A.; Gentilucci, L.; Dattoli, S.D.; Baiula, M.; Spampinato, S. M.; Giacomini, D. Targeting integrins $\alpha_v\beta_3$ and $\alpha_5\beta_1$ with new β-lactam derivatives. *Eur. J. Med. Chem.* **2014**, *83*, 284-293.
(15) Baiula, M.; Galletti, P.; Martelli, G.; Soldati, R.; Belvisi, L.; Civera, M.; Dattoli, S. D.; Spampinato S. M.; Giacomini, D. New β-lactam derivatives modulate cell adhesion and signaling mediated by RGD-binding and leukocyte integrins. *J. Med. Chem.* **2016**, *59*, 9721-9742.
(16) Cainelli, G.; Giacomini, D.; Galletti, P.; Quintavalla, A. Synthesis of novel 4-(2-oxoethylidene)azetidin-2-ones by a Lewis acid mediated reaction of acyldiazo compounds. *Eur. J. Org. Chem.* **2003**, *9*, 1765-1774.
(17) Pori, M.; Galletti, P.; Soldati, R.; Calza, L.; Mangano, C.; Giacomini, D. Azetidinone-retinoid hybrids: synthesis and differentiative effects. *Eur. J. Med. Chem.* **2013**, *70*, 857-863.
(18) Choi, C.; Li, J-H.; Vaal, M.; Thomas, C.; Limburg, D.; Wu, Y-Q.; Chen, Y.; Soni R.; Scott, C.; Ross, D. T.; Guo, H.; Howorth, P.; Valentine, H.; Liang, S.; Spicer, D.; Fuller, M.; Steine, J.; Hamilton, G. S. Use of parallel-synthesis combinatorial libraries for rapid identification of potent FKBP12 inhibitors. *Bioorg. Med. Chem. Lett.* **2002**, *12*, 1421–1428.
(19) Bolchi, C.; Valoti, E.; Fumagalli, L.; Straniero, V.; Ruggeri, P.; Pallavicini, M. Enantiomerically pure dibenzyl esters of L-aspartic and L-glutamic acid. *Org. Process Res. Dev.* **2015**, *19*, 878-883.
(20) Lynch, J. K.; Holladay, M. W.; Ryther, K. B.; Bai, H.; Hsiao, C-N.; Morton, H. E.; Dickman, D. A.; Arnold, W.; King, S. A. Efficient

asymmetric synthesis of ABT-594; a potent, orally effective analgesic. *Tetrahedron-Asymmetr.* **1998**, *9*, 2791-2794.
(21) Gentilucci, L.; Cardillo, G.; Tolomelli, A.; Squassabia, F.; De Marco, R.; Chiriano, G. Cyclopeptide analogs for generating new molecular and 3D diversity. *Comb. Chem. High T. Scr.* **2009**, *12*, 929-39.
(22) Bianchini, F.; Portioli, E.; Ferlenghi, F.; Vacondio, F.; Andreucci, E.; Biagioni, A.; Ruzzolini, J.; Peppicelli, S.; Lulli, M.; Calorini, L.; Battistini, L.; Zanardi, F.; Sartori, A. Cell-targeted c(AmpRGD)-sunitinib molecular conjugates impair tumor growth of mela-noma. *Cancer Lett.* **2019**, *446*, 25-37.
(23) Hoyos-Nogués, M.; Falgueras-Batlle, E.; Ginebra, M. P.; Manero, J. M.; Gil, J.; Mas-Moruno, C. A dual molecular bio-interface combining RGD and KRSR sequences improves osteoblastic functions by synergizing integrin and cell-membrane proteoglycan binding. *Int. J. Mol. Sci.* **2019**, *20*, E1429.
(24) Fraioli, R.; Rechenmacher, F,; Neubauer, S.; Manero, J. M.; Gil, J.; Kessler, H.; Mas-Moruno, C. Mimicking bone extracellular matrix: integrin-binding peptidomimetics enhance osteoblast-like cells adhesion, proliferation, and differentiation on titanium. *Colloids Surface B* **2015**, *128*, 191-200.
(25). Postiglione, L.; Di Domenico, G.; Ramaglia, L.; Montagnani, S.; Salzano, S.; Di Meglio, F.; Sbordone, L.; Vitale, M.; Rossi, G. Behavior of SaOS-2 cells cultured on different titanium surfaces. *J. Dent. Res.* **2003**, *82*, 692-696.
(26) Conner, S. R.; Scott, G.; Aplin, A. E. Adhesion-dependent activation of the ERK1/2 cascade is by-passed in melanoma cells. *J. Biol. Chem.* **2003**, *278*, 34548-34554.
(27) Bodary, S. C.; Mc Lean, J. W. The integrin β_1 subunit associates with the vitronectin receptor α_v subunit to form a novel vitronectin receptor in a human embryonic kidney cell line. *J. Biol. Chem.* **1990**, *265*, 5938-5941.
(28) Gupta, V.; Alonso. J. L.; Sugimori, T.; Essafi, M.; Xiong, J. P.;, Arnaout, M. A. Role of the beta-subunit arginine/lysine finger in integrin heterodimer formation and function. *J. Immunol.* **2008,** *180*, 1713-1718.
(29) Taherian, A.; Li, X.; Liu, Y.; Haas, T. A. Differences in integrin expression and signaling within human breast cancer cells. *BMC Cancer*. **2011**, *11*, 293.
(30) Huey, R.; Morris, G. M.; Olson, A. J.; Goodsell, D. S. A semiempirical free energy force field with charge-based desolvation. *J. Comput. Chem*. **2007**, *28*,1145-1152
(31) Van Agthoven, J. F.; Xiong, J. P.; Alonso, J. L.; Rui, X.; Adair, B. D.; Goodman, S. L.; Arnaout, M. A. Structural basis for pure antagonism of integrin $\alpha_V\beta_3$ by a high-affinity form of fibronectin. *Nat. Struct. Mol. Biol*. **2014**, *21*, 383-388.
(32) Nagae, M.; Re, S.; Mihara, E.; Nogi, T.; Sugita, Y.; Takagi, J. Crystal structure of $\alpha_5\beta_1$ integrin ectodomain: atomic details of the fibronectin receptor. *J. Cell Biol.* **2012**, *197*, 131-140
(33) Thinn, A. M. M.; Wang, Z.; Zhou D.; Zhao, Y.; Curtis, B. R.; Zhu, J. Autonomous conformational regulation of β_3 integrin and the conformation-dependent property of HPA-1a alloantibodies. *Proc. Natl. Acad. Sci. USA* **2018**, *115*, E9105- E9114.
(34) Lin, F. Y.; Zhu, J.; Eng, E. T.; Hudson, N. E.; Springer, T. A. β-Subunit Binding Is Sufficient for Ligands to Open the Integrin $\alpha II_b\beta_3$ Head-piece. *J. Biol. Chem.* **2016**, *291*, 4537-4546.
(35) Heckmann, D.; Meyer, A.; Marinelli, L.; Zahn, G.; Stragies, R.; Kessler, H. Probing integrin selectivity: rational design of highly active and selective ligands for the $\alpha_5\beta_1$ and $\alpha_v\beta_3$ integrin receptor. *Angew. Chem. Int. Ed.* **2007**, *46*, 3571-3574.
(36) Xiong. J.-P.; Stehle, T.; Diefenbach, B.; Zhang, R.; Dunker, R.; Scott, D. L.; Joachimiak, A.; Goodman, S. L.; Arnaout, M. A. Crystal structure of the extracellular segment of integrin $\alpha_v\beta_3$. *Science* **2001**, *294*, 339–345.
(37) Springer, T. A.; Dustin, M. L. Integrin inside-out signaling and the immunological synapse. *Curr. Opin. Cell Biol.* **2012**, *24*, 107–115.
(38) Martelli, G.; Galletti, P.; Baiula, M.; Calcinari,L.; Boschi, G.; Giacomini, D. Chiral β-lactam-based integrin ligands through Lipase-catalysed kinetic resolution and their enantioselective receptor response *Bioorg. Chem.* **2019**, *88*, 102975.
(39) Marinelli L, Meyer A, Heckmann D, Lavecchia A, Novellino E, Kessler H. Ligand binding analysis for human alpha5beta1 integ-rin: strategies for designing new alpha5beta1 integrin antagonists. *J. Med. Chem.* **2005**, *48*, 4204-4207.
(40) Lin, H. Y.; Mousa, S. A.; Davis, P. J. Demonstration of the receptor site for thyroid hormone on integrin $\alpha v\beta 3$. *Methods Mol. Biol.* **2018**, *1801*, 61-65.
(41) Zhu, J.; Zhu, J.; Springer, T. A. Complete integrin headpiece opening in eight steps. *J. Cell Biol.* **2013**, *201*, 1053-1068.
(42) Paladino, A.; Civera, M.; Belvisi, L.; Colombo, G. High Affinity vs. Native fibronectin in the modulation of $\alpha_v\beta_3$ integrin conformational dynamics: insights from computational analyses and implications for molecular design. *PLoS Comput. Biol.* **2017**, *13*, e1005334
(43) Vanderslice, P.; Biediger, R. J.; Woodside, D. G.; Brown, W. S.; Khounlo, S.; Warier, N. D.; Gundlach, C.W.4th; Caivano, A. R.; Bornmann, W. G.; Maxwell, D. S.; McIntyre, B. W.; Willerson, J. T.; Dixon, R. A. Small molecule agonist of very late antigen-4 (VLA-4) integrin induces progenitor cell adhesion. *J. Biol. Chem.* **2013**, *288*, 19414-19428.
(44) Rocha, L. A.; Learmonth, D. A.; Sousa, R. A.; Salgado, A. J. $\alpha_v\beta_3$ and $\alpha_5\beta_1$ integrin-specific ligands: from tumor angiogenesis inhibitors to vascularization promoters in regenerative medicine? *Biotechnol. Adv*. **2018**, *36*, 208-227.

Table of Content